

Role of unstable periodic orbits in phase and lag synchronization between coupled chaotic oscillators

Diego Pazó^{a)}

Grupo de Física non Lineal, Fac. de Física, Universidade de Santiago de Compostela, E-15782 Santiago de Compostela, Spain

Michael A. Zaks

Institut für Physik, Humboldt Universität zu Berlin, D-10117 Berlin, Germany

Jürgen Kurths

Institut für Physik, Universität Potsdam, D-14415 Potsdam, Germany

(Received 13 May 2002; accepted 9 September 2002; published 21 February 2003)

An increase of the coupling strength in the system of two coupled Rössler oscillators leads from a nonsynchronized state through phase synchronization to the regime of lag synchronization. The role of unstable periodic orbits in these transitions is investigated. Changes in the structure of attracting sets are discussed. We demonstrate that the onset of phase synchronization is related to phase-lockings on the surfaces of unstable tori, whereas transition from phase to lag synchronization is preceded by a decrease in the number of unstable periodic orbits. © 2003 American Institute of Physics. [DOI: 10.1063/1.1518430]

An interaction between chaotic oscillators leads to adjustment of their characteristics. Depending on the strength of the coupling, interacting subsystems can share different dynamical features. Under relatively weak coupling, only the time scales of chaotic motions get adjusted; this is known as “phase synchronization.” A stronger coupling can enforce a convergence between phase portraits: a subsystem imitates the sequence of states of the other one, either immediately (“complete synchronization”), or after a time shift (“lag synchronization”). With the help of unstable periodic orbits embedded into the chaotic attractor, we investigate transition from nonsynchronized behavior to phase synchronization and further to lag synchronization. We demonstrate that the onset of phase synchronization requires locking on the surfaces of unstable tori, and relate intermittent phase jumps to local violations of this requirement. Further, we argue that onset of lag synchronization is preceded by the disappearance of many unstable periodic orbits whose geometry is incompatible with the lag configuration. We identify orbits which are responsible for intermittent deviations from the state of lag synchronization.

I. INTRODUCTION

Synchronization is a universal phenomenon that often occurs when two or more nonlinear oscillators are coupled. Its discovery dates back to Huygens,¹ who observed and explained the effect of mutual adjustment between two pendulum clocks hanging from a common support. For coupled periodic oscillators the effect of entrainment of frequencies is well understood and widely used in applications.² The last years have witnessed the successful expansion of the basic

ideas of synchronization to the realm of chaotic dynamics.³ Since chaotic oscillations are more complicated than periodic ones, such expansion is neither obvious nor straightforward. The instantaneous state of a periodic process is adequately characterized by the current value of its phase; on the contrary, complete information about the state of a chaotic variable includes, in general, more characteristics. Different degrees of adjustment between these characteristics correspond to different kinds of synchrony: from complete synchronization where the difference between two chaotic signals virtually disappears,^{4–6} through the “generalized” synchronization where the instantaneous states of subsystems are interrelated by a functional dependence,^{7,8} to phase synchronization. In the latter case coupled chaotic oscillators remain largely uncorrelated, but the mean time scales of their oscillations coincide or become commensurate.⁹

Phase synchronization appears to be the weakest form of synchrony between chaotic systems; it does not require the coupling to be strong. In certain situations, the increase of coupling leads through the further, more ordered stage of synchronized motion: the lag synchronization.¹⁰ In this state, which precedes the complete synchronization, phase portraits of subsystems are (nearly) the same, and the plot $X_1(t)$ for a variable X_1 from the first subsystem can be obtained from the plot of its counterpart X_2 from the second subsystem by a mere time shift, $X_1(t) = X_2(t + \tau)$.

Different aspects of phase and lag synchronization have been investigated mostly from the point of view of global characteristics (Lyapunov exponents, distributions of phase jumps, statistics of violations of lag configuration, etc.). It has been found that onsets of both these kinds of synchronization are preceded by intermittent behavior; close to the threshold parameter values, the coupled subsystems remain synchronized most of the time, but these epochs of synchronization are interrupted by time intervals during which syn-

^{a)}Electronic mail: diego@fmmeteo.usc.es; http://chaos.usc.es

chronization is missing. Descriptions of pretransitional intermittencies have been given in Refs. 11–13 for the case of phase synchronization and, respectively, in Refs. 10,14,15 for lag synchronization. Below, we intend to have a closer look at the local changes which occur in the phase space of mathematical models. We concentrate on invariant sets and their restructurings which simplify dynamics by gradually transforming the nonsynchronized chaotic attractor into the coherent attractor of the phase-synchronized state and, further, into a set which corresponds to the state of lag synchronization.

To follow the evolution of the attracting set under the increase of the coupling, we trace the fate of unstable periodic orbits (UPOs) embedded into the attractor. A universal and powerful tool for the exploration of chaotic dynamics,¹⁶ unstable periodic orbits proved to be especially efficient in the context of synchronization.¹⁷ Interpretation in terms of UPOs helped to understand the onset of phase synchronization in the case of a chaotic system perturbed by an external periodic force,^{11,12} i.e., in the case of unidirectionally coupled periodic and chaotic oscillators. Below, we extend this approach to a system of two bidirectionally coupled non-identical chaotic oscillators. This situation is more complicated, since now each of the participating subsystems possesses an infinite set of UPOs. In the following section we briefly characterize the properties of unstable periodic orbits which exist in both subsystems in the absence of coupling. In Sec. III we describe changes in the structure of the attractor of the coupled system which occur in the course of the increase of the coupling strength. We interpret the onset of phase synchronization in terms of phase locking on unstable tori, and argue that transition to lag synchronization should be preceded by extinction of most of the unstable periodic orbits. In Secs. IV and V, respectively, these qualitative arguments are supported by numerical results which illustrate the role of UPOs in the intermittent bursts close to thresholds of both phase and lag synchronization.

II. PERIODIC ORBITS IN THE ABSENCE OF COUPLING

As an example, we consider the system of two coupled Rössler oscillators under the same set of parameter values for which lag synchronization was reported for the first time,¹⁰

$$\begin{aligned}\dot{x}_{1,2} &= -\omega_{1,2}y_{1,2} - z_{1,2} + \varepsilon(x_{2,1} - x_{1,2}), \\ \dot{y}_{1,2} &= \omega_{1,2}x_{1,2} - ay_{1,2}, \\ \dot{z}_{1,2} &= f + z_{1,2}(x_{1,2} - c).\end{aligned}\quad (1)$$

Below, only the coupling strength ε is treated as an active parameter; other parameters have fixed values $a = 0.165$, $f = 0.2$, $c = 10$, $\omega_{1,2} = \omega_0 \pm \Delta$ ($\omega_0 = 0.97$, $\Delta = 0.02$), respectively. Besides the original paper,¹⁰ scenarios of onset of lag synchronization in Eqs. (1) under these parameter values were discussed in subsequent publications.^{14,15,18}

In each of the subsystems, taken alone, this combination of parameters ensures chaotic oscillations [Fig. 1(a)]. Projected onto the xy plane of the corresponding subsystem,

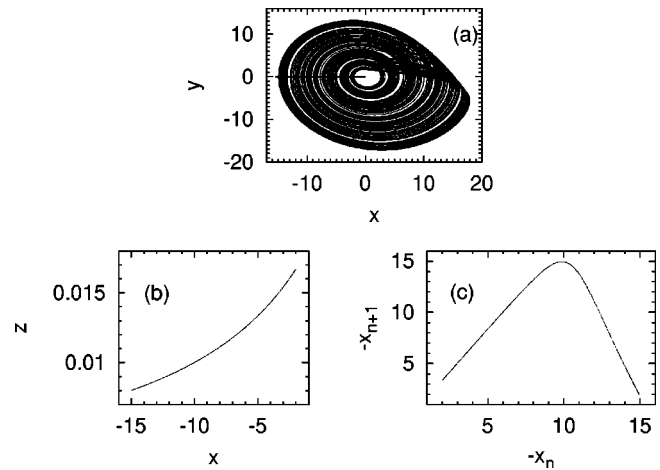


FIG. 1. Rössler oscillator at $\omega = \omega_1 = 0.99$. (a) Projection of the phase portrait; solid line: location of the Poincaré plane; (b) trace of the attractor on the Poincaré plane; (c) one-dimensional return mapping.

these oscillations look like rotations around the origin; this allows us to introduce phase geometrically, as a lift of the angular coordinate in this plane,

$$\phi_{1,2} = \arctan \frac{y_{1,2}}{x_{1,2}} + \frac{\pi}{2} \text{sign}(x_{1,2}). \quad (2)$$

The mean frequency of the chaotic oscillations is then defined as the mean angular velocity; $\Omega^{(1,2)} = \langle d\phi_{1,2}/dt \rangle$. The difference in the values of the parameters $\omega_{1,2}$ makes the mean frequencies of uncoupled oscillators slightly different: at $\varepsilon = 0$, they are $\Omega^{(1)} = 1.01926\dots$ and $\Omega^{(2)} = 0.97081\dots$, respectively. As a result, the phases of the oscillators drift apart; in order to enforce phase synchronization, the coupling should be able to suppress this drift by adjusting the rotation rates.

In order to understand the role of unstable phase orbits in the phase space of the coupled system, it is helpful to start with the classification of such orbits in the absence of coupling. In its partial subspace, each of the three-dimensional flows induces the return mapping on an appropriate Poincaré surface (it is convenient to use for this purpose the trajectories which in the i th system intersect “from above” the surface $y_i = 0$). This two-dimensional mapping is, of course, invertible; however, due to the strong transversal contraction, the trace of the attractor on the Poincaré surface is graphically almost indistinguishable from a one-dimensional curve [Fig. 1(b)]. Parameterizing this curve (e.g., by the value of the coordinate x), we arrive at the noninvertible one-dimensional map shown in Fig. 1(c). Since the latter turns out to be unimodal, its dynamics is completely determined by the symbolic “itinerary:”¹⁹ the sequence $RLL\dots$ in which the j th symbol is R if the j th iteration of the extremum lies to the right from this extremum, and L otherwise. According to numerical estimates, for $\omega = \omega_1 = 0.99$ the itinerary is $RLLLLRLLL\dots$, and for $\omega = \omega_2 = 0.95$ it becomes $RLLLLRLL\dots$. The starting segments of the two symbolic strings coincide, the first discrepancy occurs in the sixth symbol; therefore, the number of unstable periodic orbits which make l turns around origin, is the same in both sub-

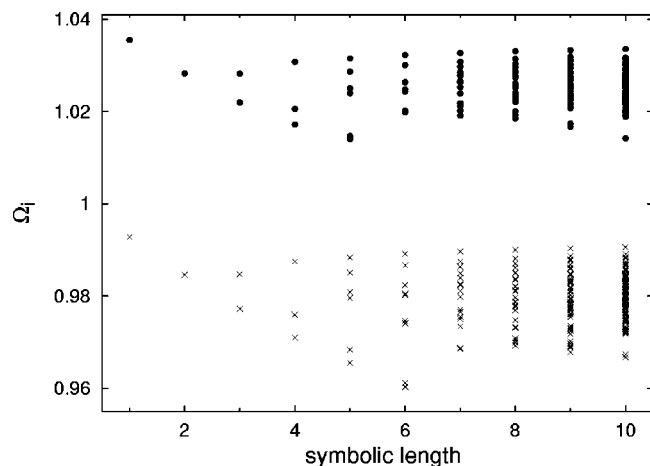


FIG. 2. Frequencies of unstable periodic orbits embedded into the attractors of the Rössler equations. Circles, $\omega = 0.99$; crosses, $\omega = 0.95$.

systems if l does not exceed 5. The number of orbits with the length $l \geq 6$ is larger in the second subsystem. Comparison of the initial 25 symbols with the symbolic itinerary of the logistic mapping $x_{i+1} = Ax_i(1-x_i)$ shows that flows with $\omega = \omega_1 = 0.99$ and $\omega = \omega_2 = 0.95$ correspond to maps with $A = 3.9904857\dots$ and $A = 3.9977031\dots$, respectively.

For our purpose we need to modify some conventional characteristics. When we consider the flow near a long periodic orbit, the duration of each single revolution (turn) in the phase space appears to be of little importance: what matters for phase dynamics, is the mean duration of the turn, i.e., the overall period of the orbit divided by the number of turns in this orbit. Below we refer to the number of turns as to the (symbolic) length of the orbit.¹² Since the time between consecutive returns onto the Poincaré plane depends on the position on this plane, the periods of all periodic solutions are, in general, different. It is convenient to characterize periodic orbits in terms of “individual frequencies” Ω_i ; these are not the usual inverse values of the corresponding overall periods, but mean frequencies per one turn in the phase space: for the orbit with period T which consists of l turns, $\Omega_i \equiv 2\pi/T$. Figure 2 presents the distributions of individual frequencies for periodic solutions for both subsystems in the absence of coupling. Since commonly the orbits with relatively short periods are sufficient for an adequate description of the whole picture,²⁰ we restrict ourselves to orbits with length $l \leq 10$; this yields 164 UPOs at $\omega = 0.99$ and 196 UPOs at $\omega = 0.95$.

As shown in Fig. 2, two frequency bands are separated by a gap. For $\omega = 0.99$ the individual frequencies belong to the interval between $\Omega_{\max}^{(1)} = 1.035519\dots$ (orbit with length 1) and $\Omega_{\min}^{(1)} = 1.014042\dots$ (one of the orbits with length 5). For $\omega = 0.95$ the values are distributed between $\Omega_{\max}^{(2)} = 0.9927899\dots$ (the same orbit with length 1) and $\Omega_{\min}^{(2)} = 0.9790416\dots$ (one of the orbits with length 6).

Besides periodic orbits, the Rössler equations possess a saddle-focus fixed point located close to the origin. Although this point does not belong to the chaotic attractor, it is not irrelevant; under coupling, it interacts with periodic orbits of the complementary subsystem and contributes to the general

scenario. To unify notation, we refer to this fixed point as the “length-0 orbit.”

III. ATTRACTOR OF THE COUPLED SYSTEM: ROLE OF UNSTABLE TORI IN SYNCHRONIZATION TRANSITIONS

Formally, at $\varepsilon = 0$ (absence of coupling) the attractor in the joint phase space of two systems contains a countable set of degenerate invariant 2-tori; direct products of each periodic orbit from the first subsystem with each periodic orbit from the second one. Again, for the purpose of comparison of phase evolution in both subsystems, it is convenient to redefine the usual notion of the rotation number on such tori; let the mean times of one revolution around the torus for the projections onto two subsystems be, respectively, τ_1 and τ_2 . Then the rotation number is introduced as the ratio $\rho = \tau_1/\tau_2$. If the equality $\rho = 1$ holds, within a sufficiently long time projections of trajectories make an equal number of rotations in the subspaces of subsystems: the torus is “phase locked.” Generalization of this interpretation for other rational values of ρ is straightforward. Obviously, at $\varepsilon = 0$, the rotation number is ω_1/ω_2 , where ω_1 and ω_2 are the individual frequencies (per one rotation, as discussed above) of the two periodic orbits which form the torus.

As soon as the infinitesimal coupling between the subsystems is introduced, the degeneracy of tori is removed. The UPOs shown in Fig. 2 produce $164 \times 196 = 32144$ tori whose rotation numbers (in the above sense) lie between $\Omega_{\min}^{(2)}/\Omega_{\max}^{(1)} = 0.92737\dots$ and $\Omega_{\max}^{(2)}/\Omega_{\min}^{(1)} = 0.97904\dots$. In general, each torus persists in a certain range of ε , and its rotation number ρ is the devil’s staircase-like function of ε : intervals of values of ε correspond to rational values of ρ .

Since the periodic orbits in subsystems are unstable, the tori are also unstable; for small values of ε , a trajectory on the toroidal surface has at least two positive Lyapunov exponents.

The boundaries of “locking intervals” of ε for each torus are marked by tangent bifurcations of periodic orbits. Such a bifurcation creates/destroys on the surface of the torus two closed trajectories, one stable (with respect to disturbances within the surface), the other one unstable. Since the motion along the torus is parameterized by the phases of subsystems, below we refer to these orbits as, respectively, “phase stable” and “phase unstable.”¹²

The following argument demonstrates that on each torus the phase-stable and phase-unstable orbits are not necessarily unique. Let the torus originate from the direct product of two periodic orbits: an UPO from the first subsystem with the length l and an UPO from the second subsystem with the length m . Then the main locking (1:1 in our notation) assumes that the phase curve is closed after n turns, n being the least common multiple of l and m . Let us take the projection of the periodic orbit onto the subspace of the first subsystem, and select some particular point on it (e.g., the highest of the n main maxima for one of the variables). By translating forwards and backwards the partial projection onto the other subsystem, we get n configurations in which one of the n maxima of the second variable is close to the selected point. Figure 3 shows such “appropriate for the

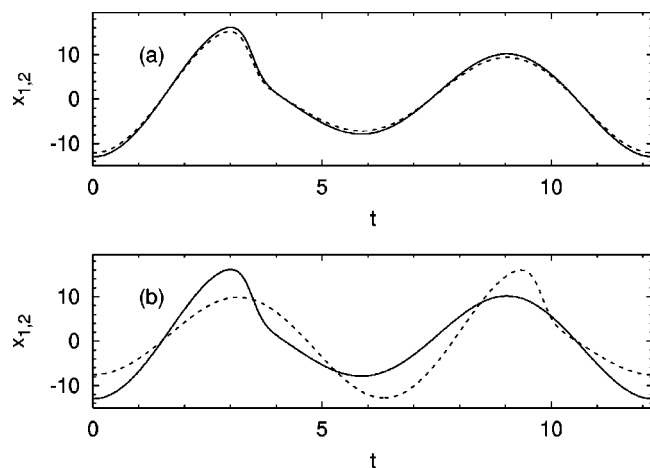


FIG. 3. Configurations favorable for the locking on the torus originated from the direct product of the UPOs of length 2: (a) “in-phase;” (b) “out-of-phase.” Solid curves, $x_1(t)$; dashed curves, $x_2(t)$.

locking” configurations for the torus generated by two orbits of length 2; in this case, $l = m = n = 2$. In general, this implies that we should expect to observe on the surface of a single torus up to n coexisting pairs of phase stable and phase unstable periodic orbits. [Naturally, the argument is not rigorous; in principle, not all of n possible configurations should necessarily be exhausted; on the other hand, the existence of additional lockings cannot be totally excluded as well.] A locking interval in the parameter space ranges from the birth of the first couple of curves with the prescribed locking ratio, to the death of the last such couple. Uniqueness of the rotation number forbids the coexistence on the same torus of periodic orbits with different locking ratios.

In the course of time a chaotic trajectory repeatedly visits the neighborhoods of unstable tori; in each of them it spends some time winding along the surface, until being repelled to some other unstable torus. During the time T spent in the vicinity of the torus with rotation number ρ , the increment of the phase difference $\phi_1 - \phi_2$ between the subsystems is $\Delta\phi \approx 2\pi(T/\tau_1 - T/\tau_2) = 2\pi(1 - \rho)/\tau_1$. Hence, unless $\rho = 1$, the passage close to a torus results in a phase drift. On the other hand, if the torus is locked in the ratio 1:1, a passage of a chaotic trajectory along one of the phase-stable UPOs on the toroidal surface leads neither to a phase gain nor to a phase loss. Therefore we can expect that in the phase synchronized state all of the tori embedded into the chaotic attractor are locked and have the same frequency ratio. From this point of view, in the course of transition to phase synchronization each of the tori present at $\varepsilon = 0$ should either reach the main locking state or disappear, from the attractor or from the whole phase space. Note that, even if a single torus within the attractor remains not locked, the ergodic nature of chaotic dynamics will ensure that from time to time the trajectory will approach this torus close enough to make the system exhibit a phase jump.

Now we proceed to lag synchronization. Let us start with ordering the UPOs in uncoupled subsystems into two sequences $\{U_i^{(k)}\}$, $k = 1, 2; i = 1, 2, \dots$. The ordering can be done by means of criteria which take into account the symbolic length and topology (expressed, e.g., by symbolic itinerary)

of the orbits. This induces labeling among the tori of the coupled system: the torus T_{ij} originates from the interaction of the orbit $U_i^{(1)}$ from the first subsystem and the orbit $U_j^{(2)}$ from the second one.

As discussed above, for the values of ε beyond the threshold of phase synchronization all the tori inside the attractor should have the same rotation number 1, hence they should possess periodic orbits. In fact, at finite values of ε neither smoothness nor even the very existence of a two-dimensional toroidal surface can be guaranteed, but this circumstance appears to be of little importance; in the synchronized state the decisive role is played not by the entire torus or its global remnants, but by relatively small segments near closed phase-stable and phase-unstable orbits. The torus may break up, but periodic orbits persist. Therefore, in our discussion below the symbol T_{ij} denotes not so much the actual two-dimensional torus, but rather the set of (possibly several) periodic orbits corresponding to the locking 1:1 on this torus. If $U_i^{(1)}$ and $U_j^{(2)}$ have symbolic lengths l and m , then their symbolic labels $A^{(1)} = RL\dots$ and $A^{(2)} = RL\dots$ consist, respectively, of l and m letters. Let n be the least common multiple of l and m . Symbolic labels $B^{(1)}$ and $B^{(2)}$ for projections of T_{ij} , respectively, onto the first and second subsystem consist of n symbols: $B^{(1)}$ is n/l times repeated $A^{(1)}$, and $B^{(2)}$ is n/m times repeated $A^{(2)}$. It can be shown, that, unless $A^{(1)} = A^{(2)}$, the labels $B^{(1)}$ and $B^{(2)}$ can neither coincide, nor be obtained from each other by cyclic permutation of symbols. The symbolic label determines the topology of the periodic orbit; in particular, it prescribes the order in which the smaller and larger turns alternate. Therefore, if symbolic labels for projections are different, there is no way to bring one of these projections very close to the other by time shift; for all values of such shift the averaged (with respect to time) difference between these projections will neither vanish nor become very small. According to this argument, only T_{ij} for which two generating UPOs have the same length and topology can persist in the attractor of lag-synchronized state. The presence of the “nondiagonal” T_{ij} is incompatible with lag synchronization. Therefore all such tori and associated closed orbits should, in the course of increase of ε , either disappear, or leave the attractor.

Further, T_{ij} with identical symbolic labels may contain several phase-stable periodic orbits. However, only the passage close to the “in-phase” orbit would allow for lag synchronization with small (compared to the mean duration of one turn) value of lag. For “out-of-phase” configurations, which are obtained from the “in-phase” by cyclic permutation of maxima, the appropriate time shift would be close to several (length of the shift) durations of the turn. Apparently, only the “in-phase” orbits contribute to the motion in the lag-synchronized state. For example, the UPO in Fig. 3(a) can participate in the lag-synchronized dynamics, whereas the UPO in Fig. 3(b) is obviously unsuitable for this purpose and, hence, should not be contained in the attractor.

Thus we expect that the onset of lag synchronization should be preceded by extinction of most of unstable periodic orbits which populate the attractor at the onset of phase synchronization. In fact, a set of two oscillators in the state of lag synchronization behaves almost the same way as one

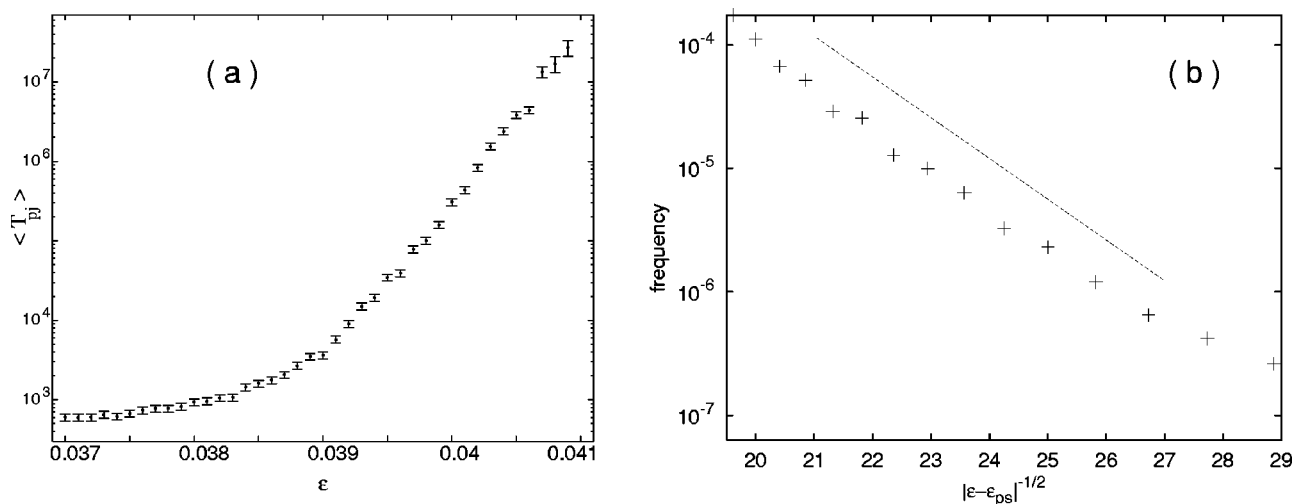


FIG. 4. Phase slips near the synchronization threshold: (a) mean time $\langle T_{pj} \rangle$ between slips versus coupling strength ε ; (b) scaling of frequency f of phase slips near ε_{ps} .

of them taken separately; in this sense, the complexity of lag synchronization is relatively low.

If the above interpretation is correct, intermittency of respective characteristics, observed below the threshold values of the coupling strength both for phase¹³ and lag synchronization^{14,15} should be caused by the passage of chaotic trajectories close to the last obstructing invariant sets. In the first case these sets are the last nonlocked tori, and in the second case they are either the last remaining UPOs from “nondiagonal” T_{ij} or the “out-of-phase” UPOs.

For completeness, it should be mentioned that there are certain UPOs which do not emerge from tori, but, instead, exist already at zero coupling. At $\varepsilon=0$ they are just direct products of steady state (fixed point) on one side, and an UPO on the other side. Obviously, such orbits are also incompatible with lag synchronization, and should disappear in the course of increase of ε .

In the following sections we test these qualitative conjectures about the mechanisms of onset of phase and lag synchronization against the numerical data obtained by integration of Eq. (1); UPOs have been computed by combination of the Schmelcher–Diakonov²¹ and Newton–Raphson methods.

IV. PHASE SYNCHRONIZATION

Phase synchronization in Eq. (1) is observed beyond the threshold value $\varepsilon = \varepsilon_{ps}$. For $\varepsilon > \varepsilon_{ps}$, the difference of phases between two oscillators remains confined within a narrow interval for $t \rightarrow \infty$; below this threshold it grows unboundedly. According to our computations, $\varepsilon_{ps} \approx 0.0416$; (this is somewhat higher than the value 0.036 reported in Ref. 10). In fact, already at $\varepsilon \geq 0.036$ the phases of two oscillators stay synchronized for most of the time; the plot of phase difference as a function of time reminds a staircase in which long nearly horizontal segments are interrupted by relatively short transitions. Such transitions (phase slips) are not instantaneous; usually it takes several dozens of turns in the phase space, in order to increase the phase difference by 2π . However, compared to the average duration of the synchronized

segment, phase slips are fast; as seen in Fig. 4, when ε approaches ε_{ps} , such duration grows from hundreds of turns through tens of thousands to millions and further on. The value 0.0416 is the highest value of ε at which we were able to observe a phase jump (only one event within $\sim 10^9$ turns of the chaotic orbit).

In the case of chaotic oscillators driven by external periodic force, the transition to phase synchronization manifests itself in the phase space as a kind of repeller–attractor collision;^{11,12,22} the local bifurcation (tangent bifurcation in which a phase-stable and a phase-unstable UPOs are born), is simultaneously the global event: disappearance of the last channel for phase diffusion. Seldom violations of synchronization below the threshold were named “eyelet intermittency,” since escapes from the phase-locked state were due to the very accurate hitting of a vicinity of the last nonlocked torus.

The same mechanism is at work in our case just below ε_{ps} ; of infinitely many tori T_{ij} embedded into the chaotic attractor, almost all are locked in the ratio 1:1. Only the passages near several remaining nonlocked (or locked in other ratios) tori can contribute to gains/losses of phase difference. Since the tori are unstable, mostly the chaotic trajectories are kicked out from their neighborhoods before producing a noticeable phase difference. Only the trajectories which come very close to the nonlocked tori, stay long enough in their vicinities in order to gain a phase slip. The frequency f of such events depends on the distribution of the invariant measure on the attractor. Assuming, for simplicity, that this measure is uniform, the same scaling law for f as in Ref. 11 can be obtained: $f(\varepsilon) \sim \exp(-1/\sqrt{\varepsilon_{ps} - \varepsilon})$. This qualitative dependence is well corroborated by our numerical data [cf. Fig. 4(b)].

Figure 5 presents the “tree” of the periodic orbits of length 1 and 2 as a function of the coupling strength ε . The vertical “amplitude” coordinate on this plot is fictitious; it plays the role of appropriately rescaled and shifted coordinate values (if actual values of coordinates were used, most

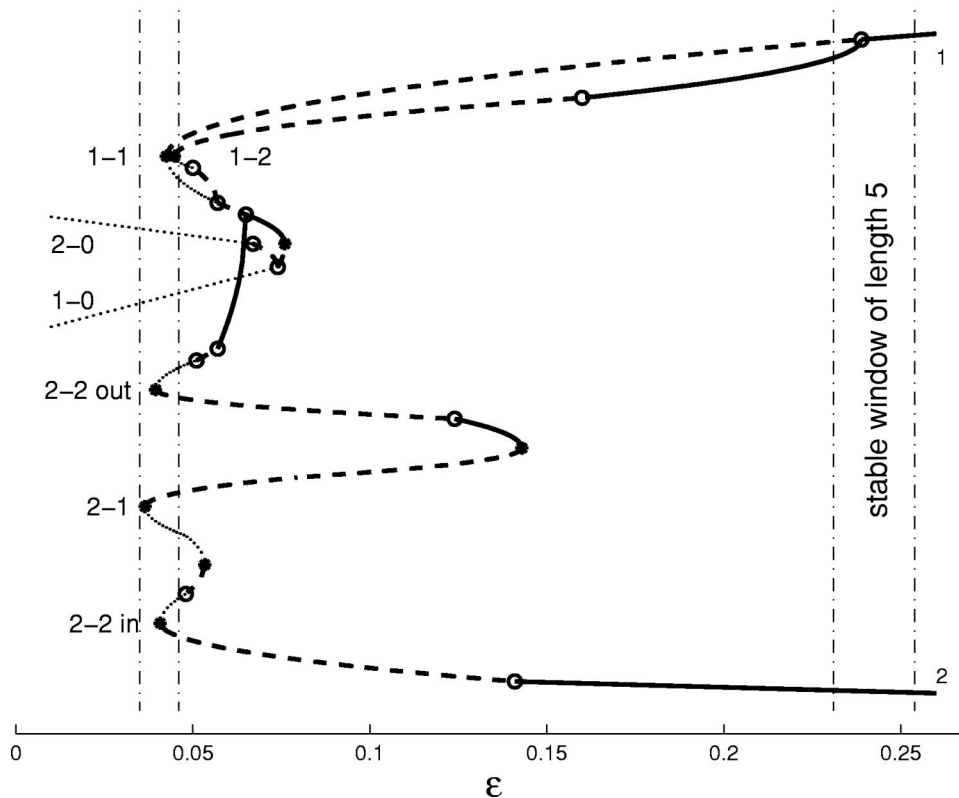


FIG. 5. Bifurcation diagram showing UPOs of length 1 and 2. Notation: *, saddle-node bifurcations; ○, period-doubling bifurcations. Solid, dashed, and dotted lines, orbits unstable in 1, 2, and 3 directions, respectively.

of the branches would overlap, strongly hampering understanding of the bifurcation sequences).

Tangent bifurcations are marked with asterisks (*), and period-doublings are denoted by small circles (○). The notation $m-m'$ stands for the locking on the torus which is the direct product of the length- m and the length- m' orbits of the first and second oscillators, respectively. Thus, the 2-2 torus undergoes two lockings: at the moment of birth of corresponding UPOs, phase lags between both oscillators, are respectively, $\sim \pi/2$ and $\sim 2\pi + \pi/2$; as ε grows, the values of these lags decrease. In accordance with the above classification, we call these orbits in- and out-of-phase lockings. It may be seen in Fig. 5 that the tangent bifurcations which create orbits of length 1 and 2, occur in a small interval around $\varepsilon = 0.04$, i.e., close to the approximate threshold of phase synchronization. At slightly higher values ($\varepsilon > 0.05$) we detect period-doubling bifurcations. The presence of period-doublings, as well as of Hopf bifurcations on other branches (see below) indicates that the smoothness of the corresponding toroidal surfaces is already lost.

Recall that label 0 denotes orbits which are born from the direct products of the steady solution with periodic solutions. The plot shows that, as expected, such orbits disappear relatively early; the branch 2-0 joins the branch 1-0 in the course of the inverse period-doubling bifurcation. The branch 1-0, in its turn, annihilates at $\varepsilon = 0.076\,736\,1$ with one of the branches born on the torus 1-1.

As a further illustration, in Fig. 6 we show solution curves and bifurcation points for orbits of length 3. This case is richer, insofar as each isolated oscillator contains two UPOs of this length (cf. Fig. 2); they are labeled 3a and 3b.

Since every orbit possesses three maxima of $x_{1,2}$, on each of the 4 emerging tori there can be up to three pairs of UPOs; along with in-phase orbits, there are two out-of-phase configurations, with phase lags $\sim 2\pi$ and $\sim 4\pi$, respectively. Now, besides tangent and period-doubling bifurcations, Hopf bifurcations (denoted by °) are also identified. In fact, it appears that Hopf bifurcations substitute some expected lockings. It should be noted that in this case all tangent bifurcations which create UPOs, occur at $\varepsilon < 0.04$.

A remarkable feature here are the isolas in Figs. 6(b) and 6(c); each family of out-of-phase lockings is not connected to families of periodic solutions and exists only in the relatively small interval of values of ε . As seen in Fig. 6(a), for sufficiently high values of ε of all the UPOs of length 3, only two in-phase orbits survive.

Several further families of UPOs are not shown on these plots. When ε is increased, the orbits of the type 0-2" disappear one-by-one in the inverse period-doubling cascade, and finally the last of them, the UPO 0-1, shrinks and merges with the fixed point of the system (in our notation, 0-0) in the inverse Hopf bifurcation. The orbits 3a-0 and 3b-0 coalesce in a saddle-node bifurcation, as well as the orbits 0-3a and 0-3b. The tori 3a-1 and 3b-1 annihilate each other in the same way as the 2π -out-of-phase lockings, 3a-3b and 3a-3a in Fig. 6(b). On the other hand, we failed to locate numerically the 1-3a and 1-3b lockings; it seems that both tori also collide and disappear in a saddle-node bifurcation (or they get locked but their UPOs survive in a very narrow range of ε).

Calculations for UPOs of other lengths have shown qualitatively similar pictures, with tangent bifurcations

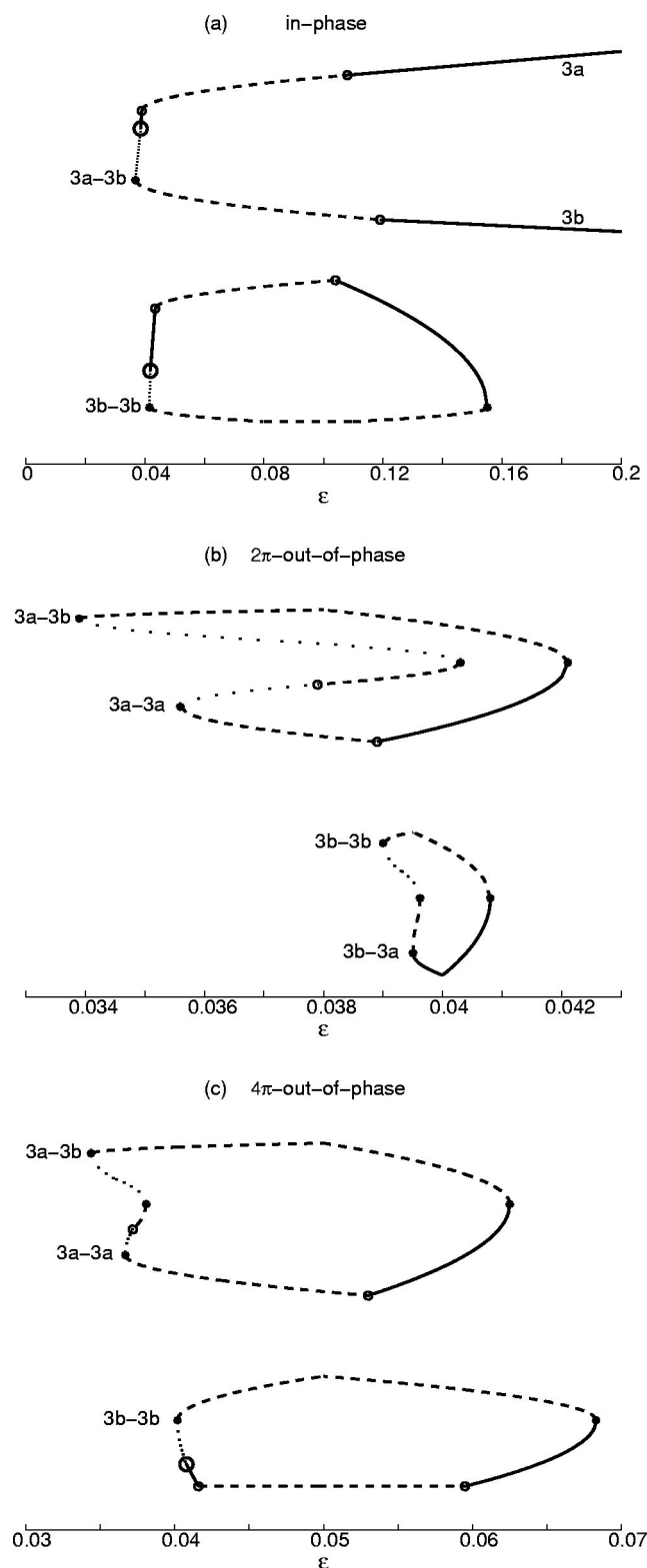


FIG. 6. Bifurcation diagram for UPOs of length 3. Notation: °, Hopf bifurcations; others as in Fig. 5.

around $\varepsilon \approx 0.04$ and short-lived out-of-phase lockings.

We have also performed numerical experiments in order to verify the conjecture that phase jumps occur when the trajectory approaches a nonlocked torus. Since we are presently unable to locate numerically in the phase space the two-dimensional unstable tori, sometimes it is difficult to

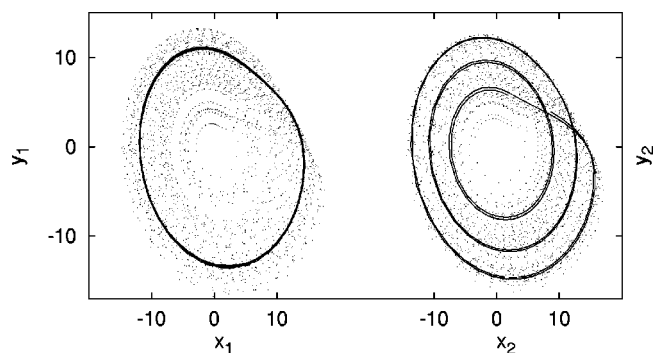


FIG. 7. A snapshot of the system at the beginning of the phase jump. $\varepsilon = 0.0409$. Dotted lines, chaotic orbit; solid lines, last six turns of the chaotic orbit.

assign the jump to the passage near a particular torus. Nevertheless, in certain cases it was possible to identify a configuration which provoked a phase jump. In such situations, in the beginning of the jump the segments of trajectories of the first and the second oscillators resemble closed orbits. An example is shown in Fig. 7, where the passage of the system close to the 1-3 torus can be recognized. In general, the further from 1 is the rotation number ρ on the degenerate torus at $\varepsilon=0$, the higher should be the magnitude of coupling required for the locking. In the frequency distribution from Fig. 2, the highest individual frequency belongs to the orbit of length 1; the tori, built with the participation of this UPO, require relatively strong coupling in order to get locked. In accordance with this, many of the phase jumps close to the threshold of phase synchronization are preceded by an approach of the first oscillator to the orbit of length 1.

Notably, the locking on the torus 1-1 occurs at the relatively high value $\varepsilon = 0.0424585$, which is above the empirically determined threshold $\varepsilon_{ps} = 0.0416$. This means that either this torus does not belong to the attractor, or the close passages happen so seldom, that one should observe the system for times higher than 10^9 mean rotation periods (our longest runs) in order to experience such jumps. We cannot point out which torus is the last one to be locked. Among the relatively short orbits, the closest to ε_{ps} locking appears to be the tangent bifurcation, which creates orbits of length 4 at $\varepsilon_{ps} = 0.0414302$.

V. LAG SYNCHRONIZATION

The lag synchronized state in Eq. (1) was found to exist above the critical value of the coupling strength $\varepsilon_{ls} \approx 0.14$.¹⁰ In this state, the dynamics of both oscillators is very similar to the one that they exhibit being isolated, but now they are related by a time lag, $x_1(t) \approx x_2(t + \tau_0)$.

The transition from phase synchronization to lag synchronization was shown to be preceded by a intermittent region where lag synchronization was interrupted by bursts.¹⁰ Since the Rössler oscillator is approximately isochronous, the time lag is practically equivalent to the phase lag. In Fig. 8(a) the value of the mean phase difference $\langle \Delta \phi \rangle$ between both oscillators is shown, as well as the corridor formed by this difference \pm its standard deviation σ . For $\varepsilon > 0.14$ this corridor is rather narrow (albeit nonzero); when ε

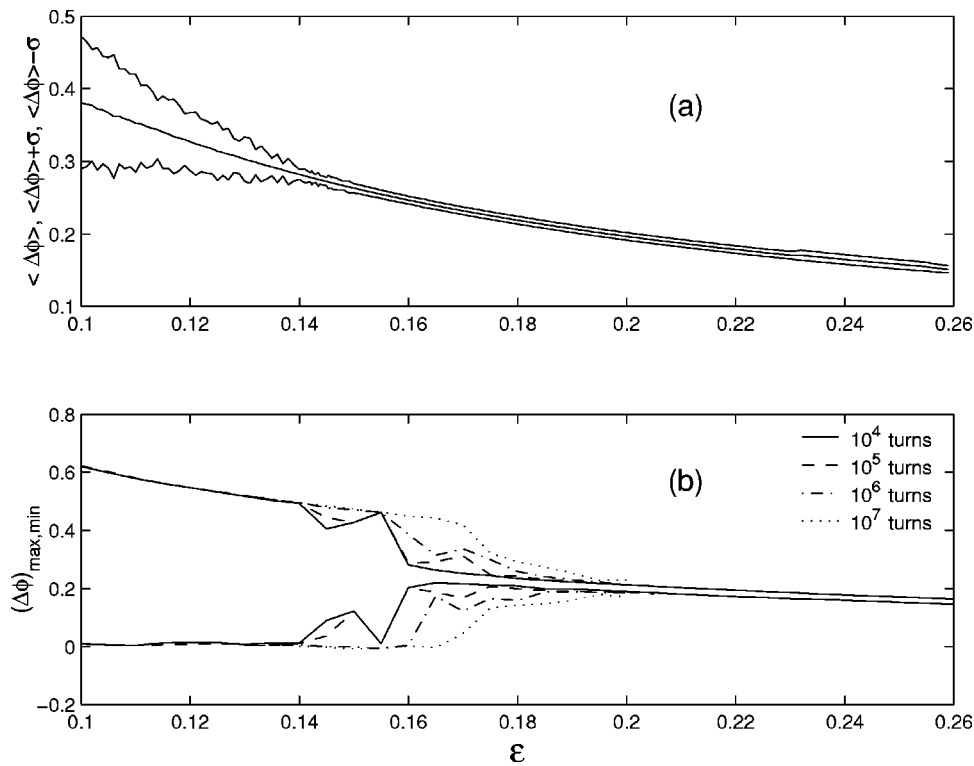


FIG. 8. (a) Mean phase difference between subsystems, and the bounds set by standard deviation. (b) Maximum and minimum phase difference computed for trajectories with different number of turns.

is decreased below 0.14, the deviation rapidly grows. However, the minimal and maximal values for deviations of phase difference from its mean value remain nonsmall also beyond $\varepsilon = 0.14$ [Fig. 8(b)]. This is a typical feature of intermittency. By increasing computing time, we were able to detect larger deviations from $\langle \Delta\phi \rangle$ at higher values of ε ; the plot shows dependencies estimated from chaotic orbits of different length.

What is the role played by UPOs in this intermittent transition to lag synchronization? We begin the discussion with the observation that growth of the coupling strength reduces the volume of phase space occupied by the attractor. Evolution of the system to this state is illustrated by return maps for one coordinate, recovered from the intersection of the attractor with the Poincaré plane $y_1 = 0$ (Fig. 9).

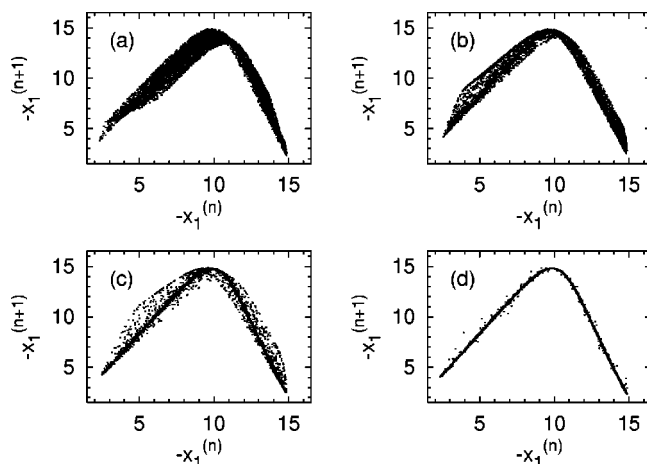


FIG. 9. Return maps for the variable x_1 on the Poincaré plane $y_1 = 0$. (a) $\varepsilon = 0.03$; (b) $\varepsilon = 0.08$; (c) $\varepsilon = 0.12$; (d) $\varepsilon = 0.14$.

As ε is increased, the initially diffuse cloud becomes more structured, with more and more points settling onto the “one-dimensional” backbone. For $\varepsilon \approx \varepsilon_{ls}$, the mapping is reminiscent of Fig. 1(c) (however, there remains a small proportion of points which lie at a distance from the parabola-like curve). Such behavior implies that the system must possess a set of UPOs similar to that of an isolated Rössler oscillator; according to Fig. 2, for $\varepsilon > \varepsilon_{ls}$ there should be one UPO of length 1, one UPO of length 2, and two UPOs of length 3. Characteristics of unstable periodic orbits for the value ε slightly beyond ε_{ls} are shown in Fig. 10. According to Fig. 10(a), correspondence with an isolated oscillator is not reached yet; the full system possesses two UPOs of length 2, as well as four orbits of length 3 and four orbits of length 4, whereas the description based on the unimodal

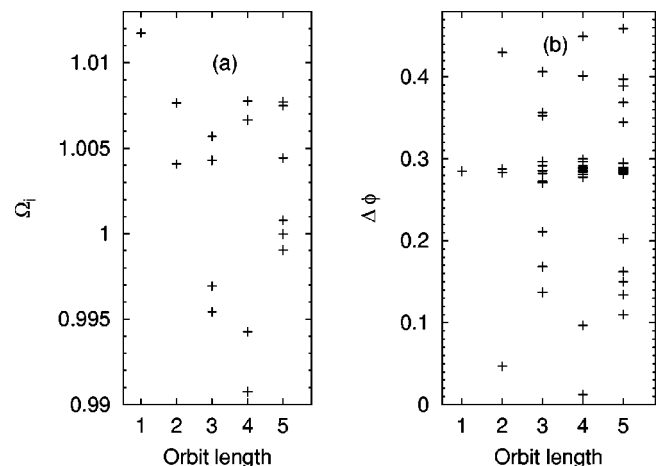


FIG. 10. Periodic orbits at $\varepsilon = 0.15$. (a) Individual frequencies Ω_i ; (b) phase lags $\Delta\phi$ on turns of periodic orbits.

mapping prescribes one orbit of length 2, not more than two orbits of length 3 and odd number (1 or 3) for UPOs of length 4.

In the course of the further increase of ε the “superfluous” orbits eventually disappear: two orbits of length 3 annihilate by means of the tangent bifurcation at $\varepsilon = 0.154\,856$; then at $\varepsilon = 0.156\,94$ a period-doubling bifurcation unifies the orbit of length 4 with the “superfluous” orbit of length 2, and finally the branch of the latter UPO (which will be separately discussed below) joins the branch of the length-1 orbit at $\varepsilon = 0.238\,92$.

The frequencies of the UPOs are distributed over the narrow range (notably, the state of phase synchronization does not necessarily assume that all these frequencies coincide). To characterize the time shift between the subsystems, we use the value of the phase lag between them at the moment of intersection of the Poincaré plane $y_2 = 0$. Since we are interested in instantaneous values, each UPO of the length l delivers l values of $\Delta\phi$. As seen in Fig. 10(b), most of the values of the phase lag belong to the narrow range between 0.27 and 0.3; however, large deviations from this range also present. Notably, most of these deviations belong to the “superfluous” orbits. As understood from Fig. 8(b), noticeable outbursts of phase difference are very rare; this means that a chaotic trajectory only seldom visits the neighborhoods of these UPOs; accordingly, their contribution into dynamics is relatively small.

Growth of ε beyond the values shown in Fig. 9 leads to the further condensation of the points of the return map onto the one-dimensional backbone; the proportion of deviations becomes smaller. It appears that in the space phase there exists a pattern (at the moment we know too little about its properties in order to label it an “invariant manifold”), which is responsible for the lag structure and on which dynamics is adequately represented by a unimodal map. This pattern is locally attracting almost everywhere, except for certain “spots;” a chaotic trajectory which hits such a spot, makes a short departure from the pattern and disturbs the lag synchronism.

Note that at large values of ε the UPOs have only one unstable direction (one characteristic multiplier outside the unit circle); this corresponds to the instability of all periodic points of the unimodal mapping. When ε is gradually decreased, the first orbit to become unstable in a second direction is the orbit of length 1 ($\varepsilon = 0.238\,92$). This bifurcation was reported in Ref. 18, where synchronization transitions for different mismatches between ω_1 and ω_2 were studied. At this critical point, the length-1 periodic orbit embedded into the “lag attractor” undergoes the period-doubling bifurcation. As a result, an orbit of length 2 is created. Tracing this new orbit down to the small values of ε we observe that it ends up as a phase-stable orbit on the torus formed by the length-1 and length-2 UPOs of decoupled subsystems; corresponding bifurcations are shown in Fig. 5. The configuration of this orbit (two approximately equal maxima in the projection onto one subsystem versus two unequal maxima in the second subsystem) is obviously incompatible with the requirements of the lag-synchronized state. Thereby, the loss of perfect lag synchronization occurs because one of the orbits

becomes unstable in the direction “transversal” to the lag pattern; in this sense, this is a kind of a bubbling-type transition.

The existence of a window of stable length-five oscillations above $\varepsilon_{(5)} = 0.231\,03$ (see Fig. 5) was not noted in previous works. The stable periodic orbit is born at $\varepsilon_{(5)}$ in the saddle-node bifurcation. Below this value the behavior, typical for the type-I intermittency is observed, and the distribution of invariant measure on the attractor is very nonuniform; the periodic orbit leaves a “ghost,” the density of imaging points is rather high in five corresponding regions of the Poincaré section, and the length-1 UPO, which lies aside from these regions, is very seldom visited. Probably, this is the reason why earlier the intermittent behavior was not observed above $\varepsilon = 0.145$.

Another interesting feature of the transition from phase to lag synchronization was reported in Ref. 14. The criterion for this transition, proposed in Ref. 10, requires the minimum of the “similarity function” $S^2(\tau) = \langle (x_2(t) - x_1(t - \tau))^2 \rangle / (\langle x_1^2(t) \rangle \langle x_2^2(t) \rangle)^{1/2}$ to vanish or nearly vanish for some τ_0 ; naturally, τ_0 is the lag duration. In Ref. 14 it was noticed that besides the main minimum at $\tau_0/T \ll 1$, the similarity function has secondary minima at $\tau \approx \tau_0 + mT$, where $m = 1, 2, \dots$, and T is close to the mean duration of one turn in the phase space. When perfect lag synchronization is lost, the magnitudes of the secondary minima of S^2 decrease. It turns out that intermittent violations of lag synchronization consist of jumps from the main lag configuration ($x_1(t) = x_2(t + \tau_0)$) to configurations of the kind $x_1(t) = x_2(t + \tau_0 + mT)$. According to Ref. 14, during the jump stage the system seems to approach a periodic orbit.

This observation confirms the above conjecture that intermittency which precedes the onset of lag synchronization, is caused by passages near the out-of-phase UPOs. Our numerical data shed more light on the nature of these jumps and allow us to identify the orbits responsible for the intermittency. According to Fig. 5, among the orbits belonging to the out-of-phase locking of two UPOs of length 2, the least unstable one (the orbit which has only one unstable direction) exists for $0.1246 < \varepsilon < 0.1426$. Temporal evolution of $x_1(t)$ and $x_2(t)$ for this orbit is shown in Fig. 11(a); phase shift is close to the duration of one turn. Figure 11(b) shows the $y_{1,2}$ -projection of this UPO embedded into the attractor. We observe that part of this orbit is “transversal” with respect to the bulk of the attractor. In the course of the intermittent bursts, chaotic trajectories which leave the bulk region, move along this UPO. During this motion the dynamics of both oscillators gets approximately correlated, and the lag between them corresponds to the time shift seen in Fig. 11(a), $\tau \approx \tau_0 + T$.

VI. DISCUSSION

Our results show that transition to phase synchronization and onset of lag synchronization between two coupled chaotic oscillators are accompanied by profound changes in the structure of the attracting set. Unstable periodic orbits serve as mediators in these processes; when the coupling strength is increased, they should, first, appear in the phase space in

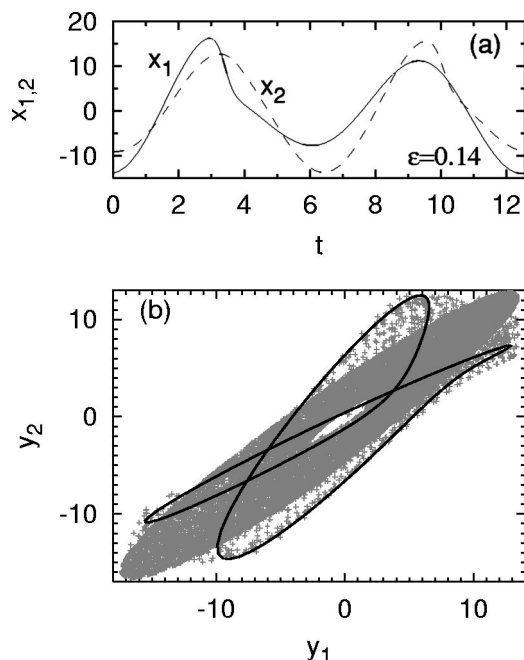


FIG. 11. Role of the out-of-phase UPO of length 2 in an intermittent lag synchronization. (a) Time series of x_1 (solid line) and x_2 (dashed line) over one period. (b) Dots, chaotic orbit on the "lag attractor" in the region of intermittent lag synchronization ($\varepsilon=0.14$); solid line, out-of-phase UPO.

order to enforce the entrainment of phases, and, second, most of them should again disappear, in order to leave in the attractor only patterns suitable for lag synchronization. Absence of necessary UPOs in the first case, and presence of "unsuitable" orbits in the second case are the reasons for intermittency. Before the onset of phase synchronization such intermittency is caused by passages near the 2-tori which are not yet locked, or locked in ratios different from 1:1; in the latter case such intermittency is, in fact, a certain form of "other" short-lived synchronization. Intermittency which precedes the onset of lag synchronization, is due to the passages near the periodic orbits, in which two oscillators are locked "out-of-phase;" such passages make the system exhibit momentary exotic lag configurations. We feel that unstable periodic orbits are an appropriate tool for the analysis of intricate details of these transitions; further numerical advances would, probably, require the technique for the calculation of unstable 2-tori.

The studied system of two coupled oscillators is nonhyperbolic, at least in the parameter region around the onset of phase synchronization. As seen in Fig. 5, an increase of ε leads to the decrease in the dimension of the unstable manifolds of UPOs. As a result, over the large intervals of ε we observe coexistence of UPOs with two-, three-, and four-dimensional unstable manifolds. In general, this phenomenon, known under the name of unstable dimension variability, has important implications for dynamics itself as well as for the validity and applicability of numerical algorithms;²³ its significance in the context of synchronization is yet to be analyzed.

ACKNOWLEDGMENTS

We benefited from stimulating discussions with S. Boccaletti, E.-H. Park, A. Pikovsky and D. Valladares. D.P. gratefully acknowledges the support by Secretaría Xeral de Investigación e Desenvolvemento of the Xunta de Galicia, and by MCyT under Research Grant No. BFM2000-0348. The research of M.Z. was supported by SFB-555. J.K. is grateful to HPR N-CT-2000-00158 and SFB-555 for the support.

- ¹Ch. Huygens (Hugenii), *Horologium Oscillatorium* (Apud. F. Muguet, Parisii, France, 1673); English translation: *The Pendulum Clock* (Iowa State University Press, Ames, 1986).
- ²I. I. Blekhman, *Synchronization in Science and Technology* (Nauka, Moscow, 1981) (in Russian); (English translation: ASME, New York, 1988).
- ³A. Pikovsky, M. Rosenblum, and J. Kurths, *Synchronization: A Universal Concept in Nonlinear Sciences* (Cambridge University Press, Cambridge, 2001).
- ⁴H. Fujisaka and T. Yamada, "Stability theory of synchronized motion in coupled-oscillator systems," *Prog. Theor. Phys.* **69**, 32–47 (1983).
- ⁵A. S. Pikovsky, "On the interaction of strange attractors," *Z. Phys. B: Condens. Matter* **55**, 149–155 (1984).
- ⁶L. M. Pecora and T. L. Carroll, "Synchronization in chaotic systems," *Phys. Rev. Lett.* **64**, 821–824 (1990).
- ⁷N. F. Rulkov, M. M. Sushchik, L. S. Tsimring, and H. D. I. Abarbanel, "Generalized synchronization of chaos in directionally coupled chaotic systems," *Phys. Rev. E* **51**, 980–994 (1995).
- ⁸L. Kocarev and U. Parlitz, "Generalized synchronization, predictability, and equivalence of unidirectionally coupled dynamical systems," *Phys. Rev. Lett.* **76**, 1816–1819 (1996).
- ⁹M. G. Rosenblum, A. S. Pikovsky, and J. Kurths, "Phase synchronization of chaotic oscillators," *Phys. Rev. Lett.* **76**, 1804–1807 (1996).
- ¹⁰M. G. Rosenblum, A. S. Pikovsky, and J. Kurths, "From phase to lag synchronization in coupled chaotic oscillators," *Phys. Rev. Lett.* **78**, 4193–4196 (1997).
- ¹¹A. Pikovsky, G. Osipov, M. Rosenblum, M. Zaks, and J. Kurths, "Attractor–repeller collision and eyelet intermittency at the transition to phase synchronization," *Phys. Rev. Lett.* **79**, 47–50 (1997).
- ¹²A. Pikovsky, M. Zaks, M. Rosenblum, G. Osipov, and J. Kurths, "Phase synchronization of chaotic oscillators in terms of periodic orbits," *Chaos* **7**, 680–687 (1997).
- ¹³K. J. Lee, Y. Kwak, and T. K. Lim, "Phase jumps near a phase synchronization transition in systems of two coupled chaotic oscillators," *Phys. Rev. Lett.* **81**, 321–324 (1998).
- ¹⁴S. Boccaletti and D. L. Valladares, "Characterization of intermittent lag synchronization," *Phys. Rev. E* **62**, 7497–7500 (2000).
- ¹⁵M. Zhan, G. W. Wei, and C.-H. Lai, "Transition from intermittency to periodicity in lag synchronization in coupled Rössler oscillators," *Phys. Rev. E* **65**, 036202 (2002).
- ¹⁶P. Cvitanović, "Periodic orbits as the skeleton of classical and quantum chaos," *Physica D* **51**, 138–151 (1991).
- ¹⁷N. F. Rulkov, "Images of synchronized chaos: experiments with circuits," *Chaos* **6**, 262–279 (1996).
- ¹⁸O. V. Sosnovitseva, A. G. Balanov, T. E. Vadivasova, V. V. Astakhov, and E. Mosekilde, "Loss of lag synchronization in coupled chaotic systems," *Phys. Rev. E* **60**, 6560–6565 (1999).
- ¹⁹P. Collet and J.-P. Eckmann, *Iterated Maps on the Interval as a Dynamical System* (Birkhäuser, Basel, 1980).
- ²⁰B. R. Hunt and E. Ott, "Optimal periodic orbits of chaotic systems," *Phys. Rev. Lett.* **76**, 2254–2257 (1996).
- ²¹P. Schmelcher and F. K. Diakonov, "General approach to the localization of unstable periodic orbits in chaotic dynamical systems," *Phys. Rev. E* **57**, 2739–2746 (1998).
- ²²E. R. Rosa, E. Ott, and M. H. Hess, "Transition to phase synchronization of chaos," *Phys. Rev. Lett.* **80**, 1642–1645 (1998).
- ²³E. Barreto and P. So, "Mechanisms for the development of unstable dimension variability and the breakdown of shadowing in coupled chaotic systems," *Phys. Rev. Lett.* **85**, 2490–2493 (2000).